

Review

# Carbon-Based Enzyme Mimetics for Electrochemical Biosensing

Esther Sánchez-Tirado , Paloma Yáñez-Sedeño \*  and José Manuel Pingarrón 

Department of Analytical Chemistry, Faculty of Chemistry, University Complutense of Madrid, 28040 Madrid, Spain; esther.sanchez@ucm.es (E.S.-T.); pingarro@quim.ucm.es (J.M.P.)

\* Correspondence: yseo@quim.ucm.es

**Abstract:** Natural enzymes are used as special reagents for the preparation of electrochemical (bio)sensors due to their ability to catalyze processes, improving the selectivity of detection. However, some drawbacks, such as denaturation in harsh experimental conditions and their rapid degradation, as well as the high cost and difficulties in recycling them, restrict their practical applications. Nowadays, the use of artificial enzymes, mostly based on nanomaterials, mimicking the functions of natural products, has been growing. These so-called nanozymes present several advantages over natural enzymes, such as enhanced stability, low cost, easy production, and rapid activity. These outstanding features are responsible for their widespread use in areas such as catalysis, energy, imaging, sensing, or biomedicine. These materials can be divided into two main groups: metal and carbon-based nanozymes. The latter provides additional advantages compared to metal nanozymes, i.e., stable and tuneable activity and good biocompatibility, mimicking enzyme activities such as those of peroxidase, catalase, oxidase, superoxide dismutase, nuclease, or phosphatase. In this review article, we have focused on the use of carbon-based nanozymes for the preparation of electrochemical (bio)sensors. The main features of the most recent applications have been revised and illustrated with examples selected from the literature over the last four years (since 2020).

**Keywords:** carbon nanozyme; artificial enzyme; enzyme mimicking; electrochemical biosensor



**Citation:** Sánchez-Tirado, E.; Yáñez-Sedeño, P.; Pingarrón, J.M. Carbon-Based Enzyme Mimetics for Electrochemical Biosensing. *Micromachines* **2023**, *14*, 1746. <https://doi.org/10.3390/mi14091746>

Academic Editors: Paulina Sierra-Rosales and Soledad Bollo

Received: 30 July 2023

Revised: 28 August 2023

Accepted: 5 September 2023

Published: 7 September 2023



**Copyright:** © 2023 by the authors. Licensee MDPI, Basel, Switzerland. This article is an open access article distributed under the terms and conditions of the Creative Commons Attribution (CC BY) license (<https://creativecommons.org/licenses/by/4.0/>).

## 1. Introduction

In 1970, Breslow and Overman [1] introduced the concept of artificial enzymes as a combination of a metal catalytic group and a hydrophobic binding cavity. More recently, this concept was extended to a variety of nanomaterials, and the name nanozyme was adopted. Among the nanomaterials described as catalysts with different enzyme activities, those functioning as peroxidase, catalase, oxidase, superoxide dismutase, nuclease, or phosphatase should be highlighted. Nowadays, these materials can be divided into two main groups: metal and carbon-based nanozymes [2]. Several advantages of nanozymes over natural enzymes, such as enhanced stability, low cost, facile production, and rapid activity, can be mentioned. These outstanding features are responsible for their widespread use in areas such as catalysis, energy, imaging, sensing, or biomedicine. Various review articles were recently published on the characteristics and applications of nanozymes. For instance, the enzyme-mimicking activities of different nanomaterials and their application to the fabrication of biosensors [3,4] and the detection of clinical biomarkers [5], as well as the applications of nanozymes in environmental monitoring [6], were reviewed. The recent progress of nanozymes in electrochemical sensing [7,8] and biosensing [9] was also reviewed.

Regarding carbon-based nanozymes, their catalytic activity has been extensively reported [10], and several examples of applications as metal-free catalysts for a variety of (bio)chemical reactions have been described [11]. Carbon nanomaterials, including fullerenes, carbon nanotubes, graphene, graphene oxide, carbon dots, graphene quantum dots, carbon nitrides, and their hybrids [12], have abundant active sites and possess special electronic and geometric properties. Furthermore, they are characterized by good stability

and biological safety, while their intrinsic enzyme activity allows them to mimic natural oxidase, peroxidase, superoxide dismutase, or catalase enzymes [7]. These nanomaterials provide additional advantages compared to metal-based artificial enzymes, such as higher stability, tuneable activity, and good biocompatibility. Progress on the use of peroxidase-like carbon-based nanozymes [13] and their biomedical applications [14] have been reviewed. More recently, Sun et al. [12] revised the design, catalytic mechanism, and bio-application of carbon nanozymes.

In this review article, we have focused on the use of carbon-based nanozymes for the preparation of electrochemical (bio)sensors. The main characteristics and advantages offered by the most recent applications have been illustrated with examples selected from the literature in the last four years (since 2020). The highlighted approaches have been ordered according to the type of carbon nanomaterial and their use as electrode modifiers or nanocarrier tags for detection, as well as the class of (bio)sensing platform. To provide complete information, the tables summarize the rationale and main features of relevant (bio)sensing devices involving carbon nanozymes applied mainly to clinical, food, and environmental monitoring.

## 2. Nanozymes Involving Carbon Nanotubes

As stated above, carbon nanotubes, graphene, and graphene oxide are some of the carbon nanomaterials whose enzymatic activity has been known for years and that have found application in the construction of electrochemical (bio)sensors. Although fullerenes have also been shown to possess enzyme-like behavior in the form of superoxide dismutase (SOD) [15], no applications based on this property have been found in the (bio)electroanalytical field. It should be noted that the enzymatic activity of fullerenes has been attributed to the existence of surface electron defect regions that promote the adsorption of  $O_2^{\cdot -}$  [16], being also dependent on the number of carboxyl groups on carboxyfullerenes [17].

Regarding carbon nanotubes, some recent and interesting applications should be noted. Song et al. [18] described the intrinsic peroxidase-like activity of single-walled carbon nanotubes catalyzing the reaction of the peroxidase substrate 3,3',5,5'-tetramethylbenzidine (TMB) in the presence of hydrogen peroxide. In addition, the effect of the different oxygenated groups on the enzymatic activity of this nanomaterial was investigated [19]. Although the advantages of these nanomaterials are significant, the main disadvantage is the relatively low enzyme activity, which has led to the design of several strategies to enhance their catalytic effects. Among them, doping with heteroatoms should be highlighted due to its effectiveness. In various configurations, carbon nanomaterials act as supports for metal nanoparticles that enhance their mimicking activity. As an example, Co nanoparticle-decorated bamboo-like N-doped carbon nanotubes (Co-bNCNTs) exhibited excellent oxidase activity, prevented self-aggregation, and exposed more active sites [20]. Moreover, the synergistic effect between CoNPs and bNCNTs could also contribute to enhancing the catalytic activity. The Co-bNCNTs/GCE sensor was applied to the determination of dopamine (DA), showing a wide detection range of 0.5–150  $\mu\text{M}$  and a low detection limit of 0.0342  $\mu\text{M}$ . The Michaelis–Menten constant,  $K_m$ , was also determined from the Lineweaver–Burk equation, which provided a value of 87.48  $\mu\text{M}$  for DA.

More recently, an oxidase-like nanozyme was prepared from boron–nitrogen-doped CNTs with encapsulated iron nanoparticles, Fe/bNCNTs [21]. Using this nanomaterial, an electrochemical sensor was fabricated for the simultaneous determination of DA and uric acid (UA) with a peak potential separation of 139 mV. The calibration curves ranged from 1 to 630  $\mu\text{M}$  (DA) and 0.5 to 2065  $\mu\text{M}$  (UA), with detection limits of 0.8 and 0.28  $\mu\text{M}$ , respectively. In addition, the proposed sensor was successfully applied to the detection of both targets in human serum. Ruthenium nanoparticles have also been utilized to prepare carbon nanotube hybrids for catalytic applications. For instance, MWCNTs/RuNPs produced a synergic effect on the non-enzymatic catalytic reduction of  $H_2O_2$ , allowing quantification in a wide linear range from 0.5  $\mu\text{M}$  to 1.75 mM. This good behavior contributed toward

developing a bienzymatic glucose biosensor in the presence of avidin and biotinylated glucose oxidase [22].

Artificial nanozymes involving carbon nanotubes combined with other nanomaterials have been extensively reported. Lin and Lin prepared a CNT-based nanozyme by cyclic voltammetric functionalization of CNTs with 2,20-azino-bis(3-ethyl-benzothiazoline-6-sulfonic acid) (ABTS). The corresponding sensor was applied to the determination of human serum albumin (HSA) in neat urine [23]. The kinetics of adsorption and the electrochemical oxidation of HSA at the modified electrodes were investigated, and a sensitive method was developed for the point-of-care diagnosis of microalbuminuria. A porous MoS<sub>2</sub>/MWCNT nanohybrid network with oxidase-like behavior was used to develop an electrochemical nanozyme sensor coupled with machine learning for the DPV detection of carbendazim (CBZ) in tea and rice [24]. Good electrocatalytic capacity and a wide linear range between 0.04 and 100 μM CBZ with an LOD value of 7.4 nM were obtained. More recently, a nanozyme with 2D/1D heterostructure was fabricated by the in situ growth of MoS<sub>2</sub> nanosheets onto single-walled carbon nanotubes (SWCNTs). The so-obtained SWCNTs@MoS<sub>2</sub> nanozyme exhibited greatly improved peroxidase-like activity due to the 2D/1D interfacial coupling, which might provide more active sites enhancing charge transferring during the catalytic reactions [25]. MoS<sub>2</sub>/MWCNTs nanostructures were prepared by our group and used as nanocarrier tags with immobilized detection antibodies for the construction of a dual immunosensor for the simultaneous determination of two cytokines, BAFF (B cell activation factor) and APRIL (a proliferation-induced signal) [26]. The peroxidase-like catalytic activity of the MoS<sub>2</sub>-based nanomaterials was positively evaluated by testing the oxidation of TMB in the presence of H<sub>2</sub>O<sub>2</sub>. However, a weak enzymatic activity was observed, and so, in order to obtain an electrochemical response high enough to reach the required sensitivity, HRP was also incorporated into the MoS<sub>2</sub>/MWCNTs conjugate. Table 1 summarizes the characteristics of the selected methods commented above as well as of other recently reported applications of carbon nanotube-based nanozymes [20,21,23,24,26].

**Table 1.** Some selected electrochemical (bio)sensors prepared with nanozymes involving carbon nanotubes.

| Enzyme-like | K <sub>m</sub> /Substrate | Configuration  | Technique   | Analyte               | LR/LOD  | Application/Sample                      | Ref. |
|-------------|---------------------------|--|-------------|-----------------------|---|---|------|
| oxidase     | 87.48 μM/dopamine         | Co/bBNCNTs/GCE   | DPV         | dopamine              | 0.5–150 μM/<br>0.0342 μM  | Clinical/<br>spiked<br>serum            | [20] |
| oxidase     | -                         | Fe/BNCNTs/GCE  | amperometry | dopamine<br>uric acid | 1–630 μM/0.8 μM<br>0.5–2065 μM/<br>0.28 μM                                    | Clinical/<br>serum                      | [21] |
| oxidase     | -                         | CNTs/ABTS/SPCE   | CV          | HSA                   | 0.15–1.50 μM/<br>60 nM  | Clinical/urine                          | [23] |
| oxidase     | -                         | MoS <sub>2</sub> /MWCNTs/<br>GCE                       | DPV         | CBZ                   | 0.04–100 μM/<br>7.4 nM  | Food/tea and<br>rice                    | [24] |
| peroxidase  | -                         | MWCNTs/MoS <sub>2</sub><br>(-HRP)-dAb<br>(nanocarrier) | amperometry | BAFF/APRIL            | 0.24–120 ng/mL/<br>0.08 ng/mL (BAFF);<br>0.19–25 ng/mL/<br>0.06 ng/mL (APRIL) | Clinical/<br>serum and<br>cell extracts | [26] |

Abbreviation: ABTS, 2,20-azino-bis(3-ethylbenzothiazoline-6-sulfonic acid); APRIL, a proliferation-inducing ligand; BAFF, B cell activating factor; BNCNTs, boron–nitrogen-co-doped carbon nanotubes; bBNCNTs, bamboo-like N-doped carbon nanotubes; CBZ, carbendazim; CV, cyclic voltammetry; dAb, detection antibody; DPV, differential pulse voltammetry; LR, linear range; and LOD, limit of detection.

### 3. Nanozymes Involving Graphene-Based Nanomaterials

Graphene oxide (GO) and reduced graphene oxide (rGO), with the two-dimensional structure of graphene, also play key roles in the nanozyme field. They have abundant surface defects and various oxygen-containing functional groups, including epoxy, hydroxyl, ether, endoperoxide, carbonyl, carboxyl, and ester, which have been reported to

display peroxidase mimicking activities. Song et al. stated that carboxyl-modified GO showed intrinsic peroxidase-like activity and applied it to the colorimetric detection of glucose [27]. GO and rGO can activate  $H_2O_2$ , generating hydroxyl radicals with higher oxidizabilities and performing POD-mimicking activities [28]. N-doping in carbon nanomaterials also selectively enhances the peroxidase-like activities of rGO, most likely due to the adjustment of the charge density and the increase in active sites [29]. As an example, Hu et al. [30] compared the kinetic parameters of the enzyme-like behavior for rGO and N-doped rGO, obtaining Michaelis–Menten constants ( $K_m$ ) of 0.5456 mM and 0.1115 mM for  $H_2O_2$ , respectively, the lower value indicating a higher affinity for the substrate.

The origin of the peroxidase-mimicking activity of graphene-based nanomaterials such as GO and rGO is not well known [28]. Some studies indicate that, among the various oxygen moieties, the carbonyl groups are the active centers. Several graphene-based hybrids have been developed for their use as nanozymes and applied to the construction of electrochemical sensors and biosensors. However, the enzymatic activity has not been demonstrated in all cases. Carboxyl-modified graphene oxide (GO-COOH) has been found to exhibit intrinsic peroxidase-like activity when catalyzing the reaction of the peroxidase substrate TMB in the presence of  $H_2O_2$  [5]. Song et al. [27] determined low Michaelis–Menten constants,  $K_m$ , of 0.0237 mM and 3.99 mM for GO-COOH using TMB or  $H_2O_2$  as the respective substrates. Accordingly, some electrochemical biosensors involving GO-COOH and GO-COOH hybrids have been developed. For instance, Dilmac and Guler [31] synthesized a nanocomposite by deposition of AuNPs onto GO-COOH, which was applied to the enzyme-free electrochemical oxidation of glucose in an alkaline medium. The sensor exhibited a wide linear range of 0.02–4.58 mM with an LOD value of 6  $\mu$ M. An artificial peroxidase-like hybrid involving hemin-rGO (H-rGO) and PdNPs was prepared and used for signal amplification in the construction of an electrochemical biosensor for the determination of glypican 3 (GPC3), an emerging biomarker of hepatocellular carcinoma (HCC) [32]. As Figure 1 shows, the H-rGO-PdNPs nanozyme was conjugated to a specific aptamer (GPC3-Apt) to establish a sandwich-type configuration. Good peroxidase activity was demonstrated by enhancing  $H_2O_2$  to reduce silver ions on the electrode surface. The amount of deposited Ag was proportional to the concentration of GPC3 with an LOD value of 3.30  $ng\ mL^{-1}$  GPC3.

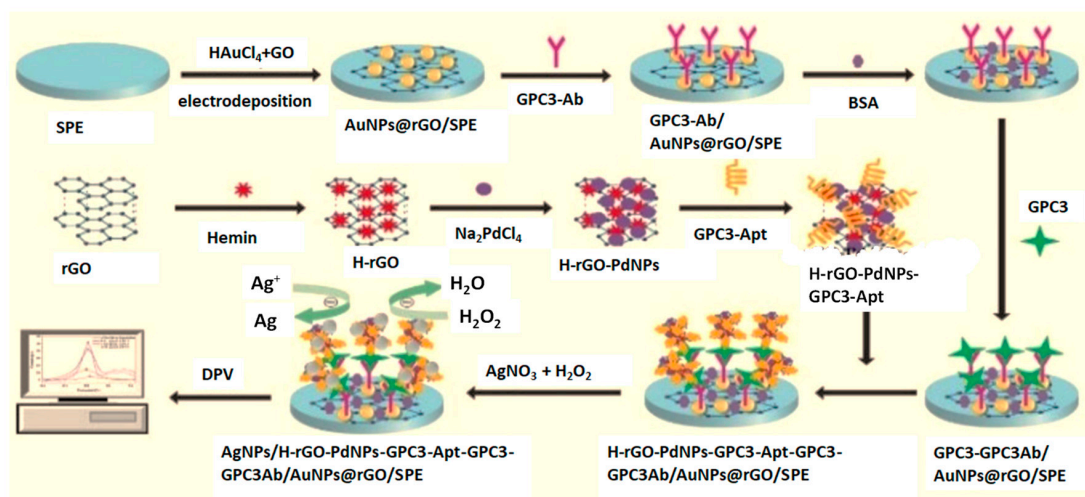


**Figure 1.** Schematic principle of the preparation of a GPC3 electrochemical nanobiosensor involving the H-rGO-Pd NPs nanozyme. Reproduced from [32] with permission.

Metallic oxides, chalcogenides, and other types of nanomaterials have also been dispersed and stabilized onto graphene derivatives to prepare nanozymes with a variety of catalytic activities. For instance, a polydopamine (PDA) surface modification-assisted pyrolysis strategy was employed to prepare CoO nanoparticle/N-doped carbon

sheets/reduced graphene oxide composites (CoONPs/N-CS/rGO). In this strategy, PDA, with abundant amine and imine moieties, served as an eco-friendly N-contained precursor and a connecting agent between the GO matrix and CoONPs [33]. Due to the high conductivity of N-CS/rGO, the synergistic catalysis between CoONPs nanoparticles and N-CS/rGO, and the intrinsic oxidase-like properties, the CoONPs/N-CS-rGO nanocomposite was used for signal amplification in the simultaneous analysis of DA and UA. The apparent Michaelis–Menten constants determined for these substrates were, respectively,  $K_m = 35.38 \mu\text{M}$  and  $51.17 \mu\text{M}$ . These relatively low values reveal its specific recognition ability toward the target molecules.

Laccase is a copper ion-containing oxidase-type enzyme that offers remarkable selectivity towards phenolic and polyphenolic substrates. Gugoasa et al. [34] prepared a AuNP/rGO hybrid laccase-like nanozyme and compared its activity to detect catechol as the target phenolic compound with that of the natural enzyme. The Michaelis–Menten constant was found to be 1.87 mM for the nanozyme deposited onto a screen-printed carbon electrode, a value slightly lower than that obtained for the native laccase, 5 mM. This result implied a stronger interaction between the substrate and AuNPs/rGO. More recently, copper nanocubes (CuNCs) were electrodeposited onto few- or multilayer graphene to obtain CuNCs-Gr/SPCE nanozyme platforms exhibiting laccase or tyrosinase-like oxidase activity. The developed nanozyme platform was used for the determination of dopamine in biological samples. The linear range was between 1 nM and 0.1 mM, and the LOD value was 0.33 nM [35].

The role of the graphene derivatives forming hybrid or artificial composite nanozymes by combination with other materials in the enzyme activity of the set is not sufficiently known. These carbon nanomaterials are good conductors and act as stabilizing agents preventing agglomeration, but exhibit weak enzyme-like activity, and thus, their contribution to the enzymatic catalysis provided by the whole nanomaterial needs to be investigated to address this knowledge towards obtaining more efficient artificial enzymes. In this sense, it is worth highlighting the work of Zhang et al. [36], who investigated the effect of rGO on the enzymatic activity of Prussian Blue nanoparticles (PBNPs), finding that the rGO structuring interface altered the properties of the nanomaterial for nanozyme-based sensing approaches. For example, electrochemical sensors using a GCE/(PB/rGO)/Nafion electrode exhibited a lower sensitivity but a wider linear range up to higher concentrations of hydrogen peroxide at pH 7.4 when compared with GCE/PB NPs/Nafion.

Table 2 summarizes the characteristics of the selected methods commented above, as well as of other recently reported applications of graphene-based nanozymes [31–40].

**Table 2.** Some selected electrochemical (bio)sensors prepared with graphene-based nanozymes.

| Enzyme-like                          | $K_m$ /<br>Substrate   | Configuration                   | Technique   | Analyte                | LR/LOD   | Application/<br>Sample          | Ref. |
|--------------------------------------|--|---------------------------------|-------------|------------------------|--|---------------------------------|------|
| oxidase                              | -  | GO-COOAuNPs/GCE                 | amperometry | glucose                | 0.02–4.48 mM/<br>6 $\mu\text{M}$   | Clinical/serum                  | [31] |
| peroxidase                           | -  | H-rGO-PdNPs-GPC3Apt/GPC3/GPC3Ab | DPV         | glypican-3             | 0.01–10.0 $\mu\text{g/mL}$ /<br>3.30 ng/mL   | Clinical/spiked serum           | [32] |
| oxidase                              | 35.38 $\mu\text{M}$ /<br>dopamine<br>51.17 $\mu\text{M}$ /UA | CoO/NCS-rGO/GCE                 | DPV         | dopamine<br>uric acid  | 0.5–110 $\mu\text{M}$ /<br>0.15 $\mu\text{M}$ /<br>1–125 $\mu\text{M}$ /<br>0.22 $\mu\text{M}$ | Clinical/spiked serum           | [33] |
| laccase                              | 1.87<br>mM/catechol  | AuNPs/rGO/SPE                   | DPV         | catechol               | 1.0 nM–1.0 mM/<br>0.33 nM  | Environmental<br>/spiked waters | [34] |
| oxidase                              | -  | CuNCs/graphene/SPCE             | DPV         | dopamine               | 0.001–100 $\mu\text{M}$ /<br>0.33 nM   | Clinical/plasma                 | [35] |
| superoxide<br>peroxidase<br>catalase | 9.2 mM/TMB   | PBNPs/rGO/GFE                   | CV          | $\text{H}_2\text{O}_2$ | 0.0012–5 mM/1.2 $\mu\text{M}$  | -                               | [36] |

Table 2. Cont.

| Enzyme-like                       | $K_m$ /<br>Substrate  | Configuration                                 | Technique   | Analyte                               | LR/LOD  | Application/<br>Sample   | Ref. |
|-----------------------------------|---|---|-------------|---------------------------------------|---|--------------------------|------|
| oxidase                           | 72.49 $\mu\text{M}/\text{X}$<br>66.84 $\mu\text{M}/\text{HX}$ | PI/graphene<br>flexible sensor                | DPV         | xanthine (X);<br>hypoxanthine<br>(HX) | 0.3–179.9 $\mu\text{M}/$<br>0.26 $\mu\text{M};$<br>0.3–159.9 $\mu\text{M}/$<br>0.18 $\mu\text{M}$ | Food/fish                | [37] |
| peroxidase                        | -   | rGO-CMC-<br>hemin@Pt/AuNPs/<br>SPCE           | DPV         | 1,5-anhidro-<br>glucitol              | 0.1–2.0 mg/mL/<br>38.2 $\mu\text{g}/\text{mL}$  | Clinical/spiked<br>serum | [38] |
| oxidase<br>peroxidase<br>catalase | 0.57 mM/ $\text{H}_2\text{O}_2$<br>0.074 mM/TMB               | PdNPs/<br>N-PC/<br>rGO/GCE                    | amperometry | glutathione                           | 70 nM–1500 $\mu\text{M}/$<br>9.8 nM   | Clinical/serum           | [39] |
| oxidase                           | -   | $\text{Fe}_3\text{O}_4/\text{MGO}/\text{ITO}$ | amperometry | glucose                               | 0.1–16 mM   | -                        | [40] |

Abbreviation: CMC, carboxymethylated chitosan; CuNCs, copper nanocubes; CV, cyclic voltammetry; DPV, differential pulse voltammetry; GPC3, glypican-3; ITO, indium tin oxide electrode; LR, linear range; LOD, limit of detection; NCS, nitrogen-doped carbon sheets; PB, Prussian Blue; PC, porous carbon; PI, polyimide; rGO, reduced graphene oxide; and TMB, 3,5,3',5'-tetramethylbenzidine.

#### 4. Nanozymes Involving Graphene Quantum Dots and Carbon Dots

The oxidase- and peroxidase-mimicking activity of graphene quantum dots (GQDs) and carbon dots (CDs) has been explored for analytical (bio)sensing using electrochemical transduction and other detection techniques. These nanozymes can replace natural peroxidase-based systems such as HRP (horseradish peroxidase)/ $\text{H}_2\text{O}_2$ , which requires labeling to a receptor for target determination, thus allowing label-free detection [41]. Both particles are defined as zero-dimensional nanomaterials showing low toxicity and biocompatibility, but unlike CDs, GQDs possess a graphene structure, which confers them the unusual properties of graphene. As in the previous section, with the aim to illustrate the importance of these nanomaterials in the construction of electrochemical (bio)sensors, several selected examples reported in the literature during recent years are summarized in Table 3 [42–53]. Although the selected examples involved electrochemical transduction, it should be noted that the number of applications using colorimetric detection where the enzymatic activity of the nanomaterial is detected by the oxidation and color change of TMB is much larger [54,55]. On the other hand, most of the reported electrochemical methods involve the use of hybridized or doped GQDs and CDs with other nanomaterials, mainly metal nanoparticles or oxides, that modulate and greatly enhance enzymatic activity.

In an interesting article, a nanocomposite of manganese dioxide and GQDs was used as a dual-functional sensing platform mimicking oxidase activity for the electrochemical and colorimetric detection of catechol (CC) and DA. The kinetic parameters were determined using TMB as the target, yielding a low  $K_m$  value of 0.11 mM. A linear relationship between the current signal and the concentration of DA and CC was obtained by DPV over the 0.5–100  $\mu\text{M}$  and 5–150  $\mu\text{M}$  ranges, with limits of detection of 0.05  $\mu\text{M}$  and 0.09  $\mu\text{M}$ , respectively [42]. The authors concluded that the electrochemical technique allowed a better sensitivity toward both analytes, with wider linear ranges, lower limits of detection, and reliability for the detection of phenolic compounds in real environmental samples. As seen in Table 2, various configurations involving AuNPs have been recently developed. AuNP/GQD nanozyme-modified electrodes contribute to the high catalytic activity and sensitivity provided by both nanocomposite elements, as is the case of the electrochemical sensor developed for the determination of quercetin by square-wave voltammetry (SWV), which provides a wide linear range of 0.1 nmol  $\text{L}^{-1}$  to  $1.0 \times 10^{-3}$  mol  $\text{L}^{-1}$  and a limit of detection of 0.033 nmol  $\text{L}^{-1}$ . The method was applied to the analysis of spiked human plasma with the advantage of requiring only a droplet of the sample [43]. More recently, GQDs synthesized by a green hydrothermal method using citric acid were modified with AuNPs and 1-amino-2-naphthol-4-sulfonic acid (ANSA) and utilized for the preparation of an electrochemical sensor for the determination of methotrexate (MTX), an anti-cancer drug [44]. The catalytic capability and synergistic effect of the ANSA/AuNP/GQD nanocomposite

deposited onto a glassy carbon electrode made possible the determination of MTX over the 0.1–100  $\mu\text{mol L}^{-1}$  linear range with an LOD value of 0.03  $\mu\text{mol L}^{-1}$ .

**Table 3.** Some selected electrochemical (bio)sensors involving graphene quantum dots and carbon dots nanozymes.

| Enzyme-like           | $K_m$ (mM)/Substrate                              | Configuration   | Technique             | Analyte                                  | LR/LOD  | Application/Sample                         | Ref. |
|-----------------------|---|---|-----------------------|--|---|--|------|
| oxidase               | 0.11/TMB  | MnO <sub>2</sub> /GQD/SPE   | DPV                   | DA, catechol                             | 0.5–100 $\mu\text{M}$ /0.05 $\mu\text{M}$<br>5–150 $\mu\text{M}$ /0.09 $\mu\text{M}$  | Environmental/waters                       | [42] |
| oxidase               | -   | AuNPs/GQDs/SPCE   | SWV                   | quercetin                                | 0.1 nM–1 mM/<br>0.033 nM  | Clinical/plasma                            | [43] |
| -                     | -   | ANSA/AuNPs/GQD/GCE  | DPV                   | MTX                                      | 0.1–100 $\mu\text{M}$ /<br>0.03 $\mu\text{M}$   | Clinical/plasma                            | [44] |
| peroxidase            | 0.056/TMB<br>0.469/H <sub>2</sub> O <sub>2</sub>  | AuNPs/N-GQDs-PEI-MOF/GCE;<br>GOx/AuNPs/N-GQDs-PEI-MOF/GCE                             | amperometry           | H <sub>2</sub> O <sub>2</sub><br>glucose | 5 $\mu\text{M}$ –1 mM;<br>2–10 mM/3.38 $\mu\text{M}$<br>(H <sub>2</sub> O <sub>2</sub> );<br>2–10 $\mu\text{M}$ ; 0.02–3 mM;<br>0.7 $\mu\text{M}$ (glucose) | Clinical/serum                             | [45] |
| undefined             | -   | anti-cTnI-AuNPs@GQDs/SPGE   | SWV                   | cTnI                                     | 1–1000 pg mL <sup>-1</sup> /<br>/0.1 pg mL <sup>-1</sup>  | Clinical/serum                             | [46] |
| peroxidase            | 0.0196/TMB<br>34.76/H <sub>2</sub> O <sub>2</sub> | AuNPs/N-CDs/GCE   | CV; amperometry       | H <sub>2</sub> O <sub>2</sub>            | -   | -  | [47] |
| peroxidase            | -   | B-CDs-AuNPs/AuE   | amperometry           | ompA;<br><i>C. sakazakii</i>             | 0.001–10 pM/<br>0.04 fM (ompA)<br>7.8–7.8 $\times 10^6$ CFU mL <sup>-1</sup><br>2.6 CFU mL <sup>-1</sup>  | Food/infant formula                        | [48] |
| peroxidase            | -   | Ti <sub>2</sub> CxMxenes/Ag <sub>2</sub> S<br>CDs/ITO                                 | photoelectrochemistry | microRNA-155                             | 1–10,000 fM/<br>/0.83 fM  | Clinical/serum                             | [49] |
| peroxidase            | -   | MIP/Fe <sub>3</sub> O <sub>4</sub> /CDs<br>@Ag-MOF/AuE<br>paper-based<br>microfluidic | DPV                   | parathion-methyl                         | 0.05–20 nM/<br>0.0116 nM  | Food, environmental/foods, soil, and water | [50] |
| peroxidase            | -   | PDDA/CuO/CDs/SPCE   | amperometry           | glucose                                  | 0.5–2 mM;<br>2–5 mM/0.2 mM  | Clinical/spiked serum                      | [51] |
| peroxidase            | 67.2/H <sub>2</sub> O <sub>2</sub>                | Fe <sub>3</sub> O <sub>4</sub> /CeO <sub>2</sub> /CDs/MWCNTs/ILs                      | CV                    | H <sub>2</sub> O <sub>2</sub>            | 0.02–1.0 $\mu\text{M}$ /0.02 $\mu\text{M}$  | -  | [52] |
| peroxidase<br>oxidase | 0.64/TMB<br>10.23/H <sub>2</sub> O <sub>2</sub>   | Co <sub>9</sub> S <sub>8</sub> /CDs/GCE   | CV                    | H <sub>2</sub> O <sub>2</sub>            | 0.1; 0.5 mM   | -  | [53] |

Abbreviations: ANSA, 1-amino-2-naphthol-4-sulfonic acid; B-CDs, boron-doped carbon dots; CV, cyclic voltammetry; ILs, ionic liquids; MIP, molecularly imprinted polymer; MOF, metal organic frameworks; MTX, methotrexate; PDDA, polydiallyl-dimethyl-ammonium; PEI, polyethyleneimine; and SWV, square-wave voltammetry.

Metal–organic frameworks (MOFs) are characterized by a large specific surface area, a high number of well-dispersed active sites, and controllable functionalities and porosity [56]. These properties make MOFs to be used as efficient supports for catalysts immobilization and enzymatic regulation [57]. As an example, a nanocomposite of nitrogen-doped GQDs and AuNPs (AuNPs/N-GQDs) with high peroxidase mimicking activity was anchored on the surface of a polyethyleneimine-functionalized MOF (P-MOF) which provided a large surface area for AuNP loading and facilitated the contact between the active sites and the electrode surface. A typical Michaelis–Menten behavior using TMB or H<sub>2</sub>O<sub>2</sub> was found for the AuNP/N-GQD nanozymes, with apparent  $K_m$  constants of 0.056 and 0.469 mM, respectively, suggesting strong affinity toward the target molecules [45]. Interestingly, the high peroxidase-like activity and large specific surface area of AuNPs/N-GQDs-P-MOF allowed the preparation of a nanocarrier for glucose oxidase (GOx) by immobilizing the enzyme to achieve a cascade reaction amplification for glucose detection (Figure 2). The intermediate by-product (H<sub>2</sub>O<sub>2</sub>) generated from the enzymatic glucose oxidation can be decomposed into H<sub>2</sub>O and oxygen in the presence of AuNP/N-GQD nanozyme. Then, the oxygen can be re-used in the enzymatic glucose oxidation to increase the reaction rate. The amplified amperometric glucose biosensor showed an LOD value of 0.7  $\mu\text{M}$  [45].

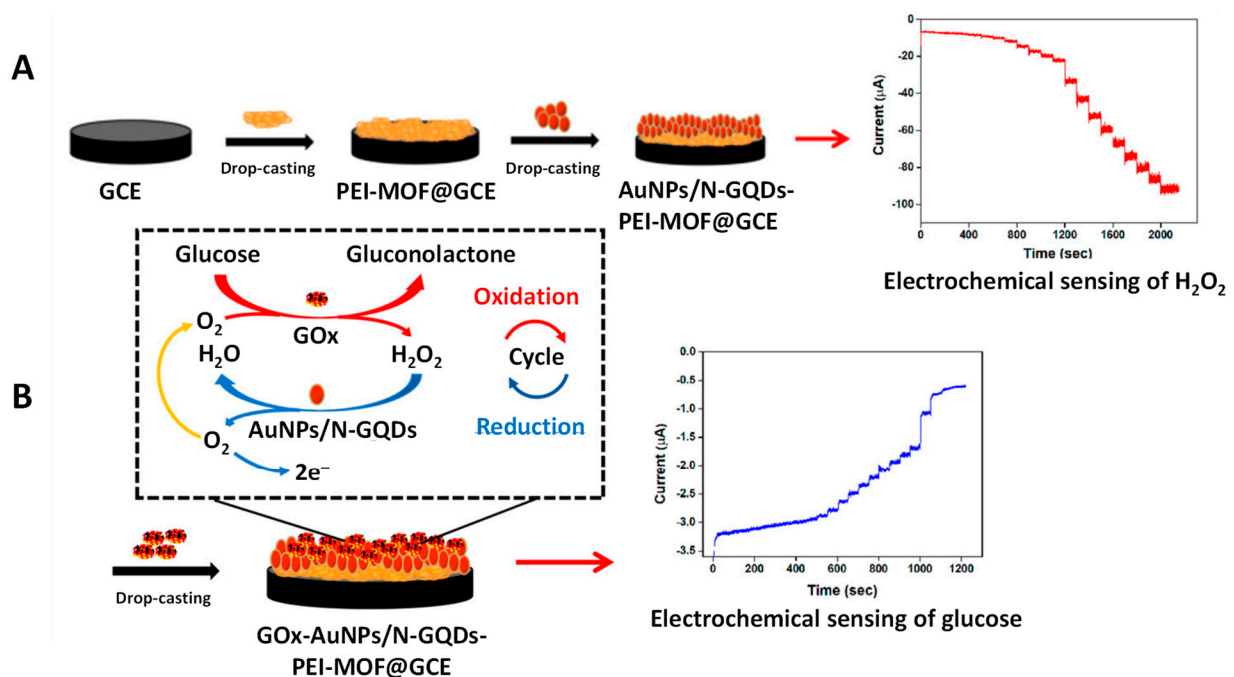


**Figure 2.** Illustration of the preparation procedure and sensing mechanism of AuNP/N-GQDs-PEI-MOF/GCE- and GOx/AuNP/N-GQDs-PEI-MOF/GCE-based amperometric sensors for (A) H<sub>2</sub>O<sub>2</sub> and (B) glucose. Reproduced from [45] with permission.

CDs are excellent nanomaterials for the preparation of hybrids or composites with enzyme-mimicking activity due to their easy surface modification and doping with heteroatoms [58,59]. The resulting nanozymes have been shown to exhibit oxidase, catalase, and superoxide dismutase, among other catalytic functions. The recent progress in CDs-based nanozymes for chemosensing and biomedical applications was reviewed by He et al. [60]. A variety of designs involving different combined nanomaterials to enhance the enzyme-like activity, as well as the electrocatalytic effects and sensitivity, have been reported in recent years for their use in the preparation of electrochemical (bio)sensors. As an interesting application, a biosensor for the detection of virulence outer membrane protein A (ompA) gene of *Cronobacter sakazakii* (*C. sakazakii*) was developed based on the peroxidase-mimicking activity of boron-doped carbon dots–Au nanoparticles (B-CDs–AuNPs) and a signal amplification strategy of exonuclease III (Exo III)-assisted target-recycling. The electrochemical response was obtained from the reduction of H<sub>2</sub>O<sub>2</sub> catalyzed by B-CDs–AuNP nanozyme and provided a high sensitivity with a broad linear range from 0.001 to 10 pmol L<sup>-1</sup> and a limit of detection as low as 0.01 fmol L<sup>-1</sup>. Interestingly, the biosensor was applied to the direct detection of extracted DNA from *C. sakazakii*, obtaining a linear semilogarithmic calibration plot between 7.8 and 7.8 × 10<sup>6</sup> CFU mL<sup>-1</sup> and an LOD value of 2.6 CFU mL<sup>-1</sup>. The developed method was applied to the determination of ompA gene segments in contaminated infant formula [48].

A photoelectrochemical biosensor involving multifunctional Au@Ag@CDs peroxidase nanoenzymes coupled with Ti<sub>2</sub>C/Ag<sub>2</sub>S composites was developed for the detection of microRNA [49]. As Figure 3 shows, after immobilization of a hairpin subsidiary probe (S1) onto the Ti<sub>2</sub>C/Ag<sub>2</sub>S surface, the target microRNA-associated bipedal DNA performed the opening of S1 to form triple helix molecules. Then, the Au@Ag@CDs were introduced into the biosensing platform through target-induced triple helix molecules. The Au@Ag@CDs nanocomposite acted as a multifunctional signal amplifier, which exhibited a synergistic catalytic effect as a peroxidase nanoenzyme. Based on the plasmonic Au@Ag@CDs nanoenzymes coupled with Ti<sub>2</sub>C/Ag<sub>2</sub>S composites, microRNA-155 was detected within a wide 1–10,000 fmol L<sup>-1</sup> linear range with a low limit of detection of 0.83 fmol L<sup>-1</sup>.

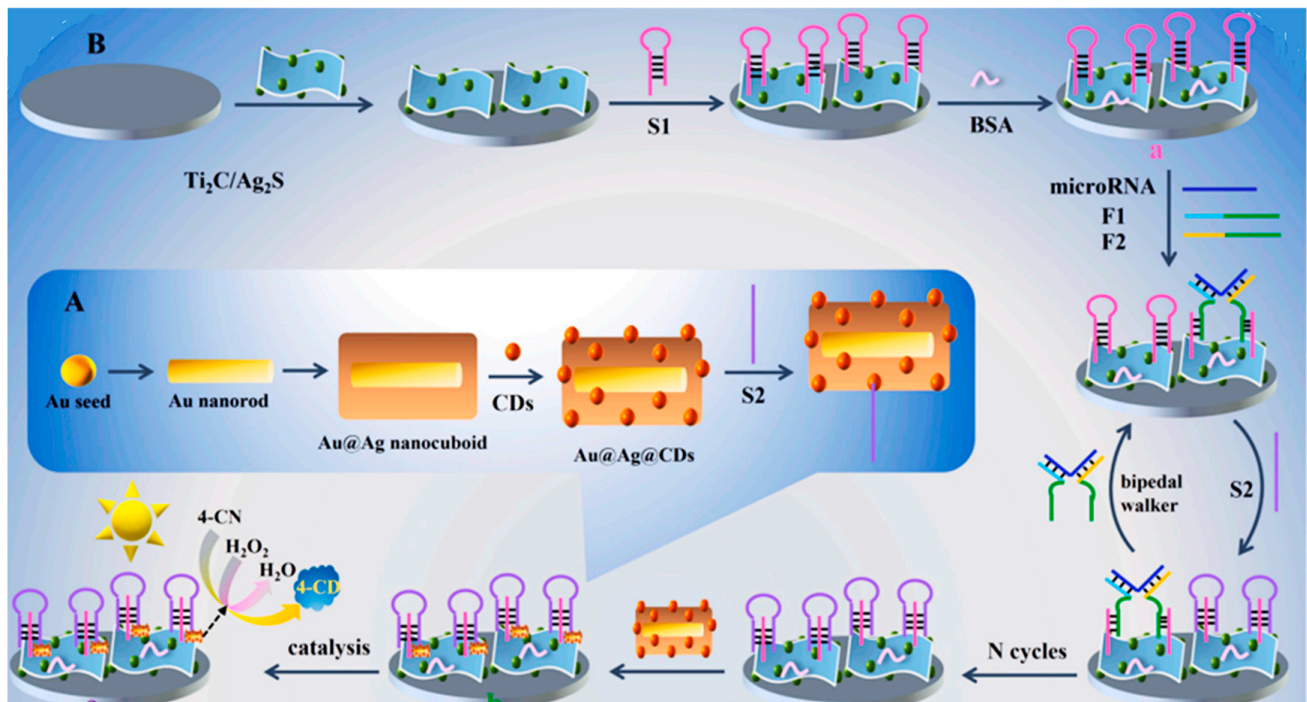


**Figure 3.** (A) Schematic display of the preparation of Ag@Ag@CDs; (B) Au@Ag@CDs nanoenzymes-driven multifunctional signal amplification combined with Ti<sub>2</sub>C/Ag<sub>2</sub>S composites for photoelectrochemical biosensing. Reprinted and adapted from [48] with permission.

Li et al. [50] proposed a double catalytic amplification strategy combining Fe<sub>3</sub>O<sub>4</sub>/CDs nanozymes and Ag-MOFs for the preparation of an electrochemical microfluidic paper-based chip to detect parathion-methyl (PM). In addition to the enzymatic catalysis coupled with the amplification of the response promoted by both components, the authors designed a molecularly imprinted polymer (MIP) using PM as a template molecule for improving selectivity. The sample introduced into the reaction zone was captured by the MIP, and a reduction current at  $-0.53$  V was generated from the target in the presence of hydrogen peroxide, which was detected at a gold electrode. A mechanism for the double amplification effect was proposed in which the catalyzed oxidation of H<sub>2</sub>O<sub>2</sub> produces several electrons and protons whose presence accelerated the reduction reaction of PM to attain a larger current and provide a detection limit of around  $10 \text{ pmol L}^{-1}$ .

Table 3 shows that other nanomaterials, such as metal oxides [51,52] and sulfides [53], combined with carbon dots have been proposed as nanozymes for the construction of electrochemical (bio)sensors. As an example, Honarasa et al. [52] prepared a triple nanozyme configuration involving Fe<sub>3</sub>O<sub>4</sub>, CeO<sub>2</sub>, and CDs exhibiting horseradish peroxidase-like catalytic activity with a Michaelis–Menten constant as low as  $67.2 \text{ mM}$  using H<sub>2</sub>O<sub>2</sub> as substrate. On the other hand, ultrasmall Co<sub>9</sub>S<sub>8</sub> nanocrystals stabilized on CDs have been synthesized, resulting in nanocomposites with a rich pore structure and outstanding bifunctional performances to mimic the catalytic activity of peroxidase and oxidase (Figure 4). The Michaelis–Menten curves for peroxidase-like activity towards H<sub>2</sub>O<sub>2</sub> provided  $K_m$  and  $V_{max}$  values of  $10.23 \text{ mM}$  and  $6.05 \times 10^{-8} \text{ M s}^{-1}$ , respectively. Likewise, the oxidase-like activity was evaluated using TMB as substrate with respective  $K_m$  and  $V_{max}$  values of  $0.123 \text{ mM}$  and  $2.38 \times 10^{-8} \text{ M s}^{-1}$  [53].

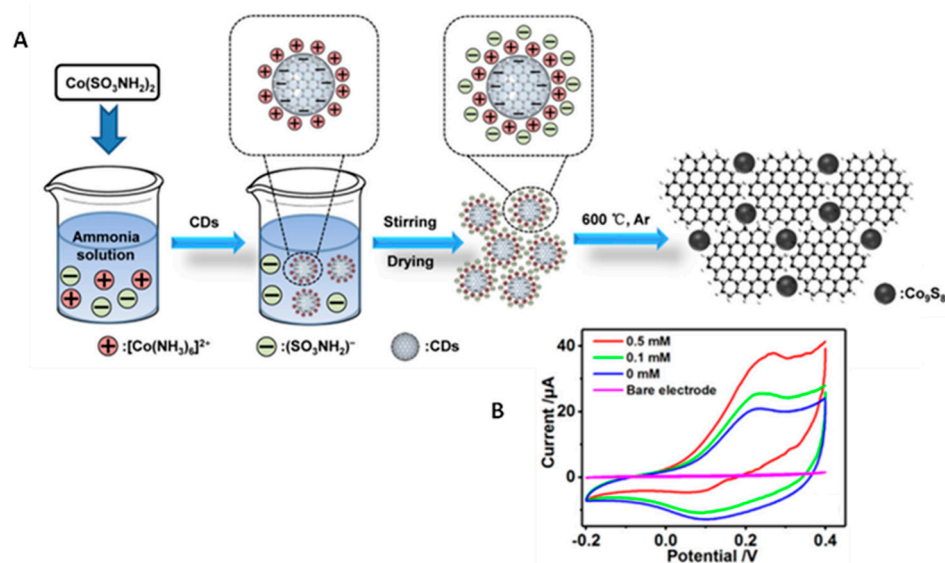


**Figure 4.** (A) Schematic illustration of the preparation of  $\text{Co}_9\text{S}_8/\text{CDs}$  and (B) cyclic voltammograms obtained at  $\text{Co}_9\text{S}_8/\text{CDs}/\text{GCE}$  with different concentrations of  $\text{H}_2\text{O}_2$ . Reprinted and adapted from [53] with permission.

## 5. Nanozymes Involving Graphitic Carbon Nitride

Graphitic carbon nitride ( $\text{g-C}_3\text{N}_4$ ) is a metal-free 2D layered material composed of carbon and nitrogen, showing structural and functional resemblance to graphene and similar physical and chemical properties, although having superior biocompatibility, thermal stability, and solubility [61,62]. The nanosheets with stacked two dimensions, the  $\text{sp}^2$  hybridized N atoms in the tri-s-triazine and surface amino-groups, and the unique chemical and physical properties have resulted in its widespread use in various sensing applications [63,64]. This carbon-based nanomaterial has been utilized to create highly active nanozymes for biosensing applications [65]. These mimicking enzymes have abundant pyridinic nitrogen moieties and a  $\pi$ -conjugated framework that provides potential binding sites for further modifications to enhance their catalytic activity [66]. Indeed,  $\text{g-C}_3\text{N}_4$  nanosheets have been shown to possess peroxidase-like activity, which has attracted attention not only in the field of sensors but also in the antibacterial area [67]. Furthermore, as seen for other carbon nanozymes, the catalytic performance of  $\text{C}_3\text{N}_4$  nanosheets as artificial peroxidases has been improved by doping with other nanomaterials [13]. Several colorimetric applications based on the enzymatic activity of  $\text{gC}_3\text{N}_4$  by TMB oxidation and color development have been reported [68,69]. However, few examples of electrochemical applications based on this activity have been found. Owing to its peroxidase-like activity,  $\text{gC}_3\text{N}_4$  has been utilized as an artificial enzyme tag for signal amplification in electrochemical detection systems, the catalytic reaction leading to significant enhancement in voltammetric/ampereometric signals [70]. Moreover, due to the strong electron-donating nature, this nanomaterial has a high electrocatalytic activity [71], so this property has been mainly exploited to anchor species and increase the selectivity in the design of electrochemical (bio)sensors. Table 4 summarizes the main characteristics of selected electrochemical (bio)sensors involving  $\text{gC}_3\text{N}_4$  [72–84]. A hybrid nanozyme consisting of in situ growing PtNPs on  $\text{gC}_3\text{N}_4$  nanosheets with enhanced peroxidase-mimicking catalytic activity was prepared. Electrochemical experiments by cyclic voltammetry were performed to investigate the peroxidase-mimicking activity toward  $\text{H}_2\text{O}_2$  [72]. Similarly, amperometry was used to study the performance and mechanism of peroxidase-like activity of oxygen-doped carbon nitride [73]. The electrocatalytic activity of  $\text{gC}_3\text{N}_4$  with respect to its morphology was also investigated by studying the oxidation of ascorbic acid and dopamine and the reduction of hydrogen peroxide [85].

**Table 4.** Some selected electrochemical biosensors involving graphitic carbon nitride (gC<sub>3</sub>N<sub>4</sub>) nanozymes.

| Enzyme-like | K <sub>m</sub> (mM)<br>Substrate                 | Configuration   | Technique                  | Analyte                       | LR/LOD  | Application/<br>Sample        | Ref. |
|-------------|--|---|----------------------------|-------------------------------|---|-------------------------------|------|
| oxidase     | 0.105/H <sub>2</sub> O <sub>2</sub><br>0.446/TMB | PtNPs@gC <sub>3</sub> N <sub>4</sub> /<br>GCE   | CV                         | H <sub>2</sub> O <sub>2</sub> | -   | -                             | [72] |
| peroxidase  | 0.098/TMB<br>0.44/H <sub>2</sub> O <sub>2</sub>  | O-gC <sub>3</sub> N <sub>4</sub>  | amperometry                | H <sub>2</sub> O <sub>2</sub> | -   | -                             | [73] |
| peroxidase  | 116/glucose                                      | ZnO/Pt/<br>gC <sub>3</sub> N <sub>4</sub> /AuE  | amperometry                | glucose                       | 0.25–110 mM/0.1 mM  | Clinical/serum<br>urine blood | [74] |
| -           | -  | MB/Au@Pt-Apt-<br>SMZ-Ab1-<br>AuOct/PEI/<br>cC <sub>3</sub> N <sub>4</sub> /AuE                | SWV                        | SMZ                           | 0.1 pg mL <sup>-1</sup> –100 ng mL <sup>-1</sup><br>0.069 pg mL <sup>-1</sup> | Food/milk                     | [75] |
| -           | -  | MNPs/CS/<br>gC <sub>3</sub> N <sub>4</sub> /CDH/GCE   | amperometry                | lactose                       | 0.9–100 mM/0.3 mM   | Food/milk<br>products         | [76] |
| peroxidase  | 0.022/TMB<br>0.136/H <sub>2</sub> O <sub>2</sub> | MNPs/cAb1-PSA-<br>Ab2/C <sub>3</sub> N <sub>4</sub><br>@LUM/NMF/NPGE                          | ECL                        | PSA                           | 10 <sup>-4</sup> –60 ng mL <sup>-1</sup> /<br>0.02 pg mL <sup>-1</sup>        | Clinical/spiked<br>plasma     | [77] |
| peroxidase  | -  | MNP/anti-5mc<br>rGO/PGE DNA   | ECL                        | methylated<br>DNA             | 20 pg–20 ng/10 pg   | Clinical/plasma               | [78] |
| peroxidase  | -  | gC <sub>3</sub> N <sub>4</sub> /BN/GCE  | amperometry                | HQ                            | 0.02–0.08 μM;<br>0.09–0.17 μM/0.009 μM  | Environmental/<br>waters      | [79] |
| peroxidase  | -  | Ag/gC <sub>3</sub> N <sub>4</sub> /GCE  | DPV                        | HQ                            | 0.99–999.96 μM/5.8 μM   | Environmental/<br>waters      | [80] |
| peroxidase  | -  | Ag <sub>2</sub> S/Ag/ZnIn <sub>2</sub> S <sub>4</sub> /<br>C <sub>3</sub> N <sub>4</sub> /FTO | photo-<br>electrochemistry | telomerase<br>activity        | 50–5 × 10 <sup>5</sup> cells mL <sup>-1</sup> /<br>19 cells mL <sup>-1</sup>  | Clinical/HeLa<br>cells        | [81] |
| peroxidase  | -  | CoOOH/gC <sub>3</sub> N <sub>4</sub> /<br>CuInS <sub>2</sub> /FTO                             | photo-<br>electrochemistry | CEA                           | 0.02–40 ng mL <sup>-1</sup> /<br>5.2 pg mL <sup>-1</sup>                      | Clinical/serum                | [82] |
| -           | -  | MIP/GQDs/<br>B-gC <sub>3</sub> N <sub>4</sub> /GCE  | DPV                        | BPA                           | 0.01–1 nM/3 pM  | Food/orange<br>juice          | [83] |
| -           | -  | anti-<br>AFB1/Thi/gC <sub>3</sub> N <sub>4</sub> /<br>ITO                                     | CV                         | AFB1                          | 1 fg mL <sup>-1</sup> –1 ng mL <sup>-1</sup> /<br>0.328 fg mL <sup>-1</sup>   | -                             | [84] |

Abbreviations: Ab1, capture antibody; Ab2, detection antibody; AFB1, aflatoxin B1; cC<sub>3</sub>N<sub>4</sub>, carboxylated carbon nitride; CDH, cellobiose dehydrogenase; CEA, carcinoembryonic antigen; HQ, hydroquinone; LUM, luminol; MNPs, magnetic nanoparticles; NMF, NH<sub>2</sub>-MIL(53)-Fe; PEI, poly (ethylenimine); PGE, pencil graphite electrode; PSA, prostate-specific antigen; SMZ, sulfamethazine; SWV, square wave voltammetry; and Thi, thionine.

An electrochemical glucose sensor was prepared by Imram et al. [74] involving a gold electrode modified with ZnO/Pt/g-C<sub>3</sub>N<sub>4</sub>, where the enzyme-like activity of g-C<sub>3</sub>N<sub>4</sub> was enhanced by doping with Pt and ZnO nanoparticles. These nanomaterials provided hydroxyl groups promoting the electrocatalysis in a neutral physiological buffer solution. The sensor exhibited a wide linear range from 0.25 to 110 mM of glucose and a good reproducibility in whole blood, which makes it suitable for diabetes monitoring. In other applications, the properties of g-C<sub>3</sub>N<sub>4</sub> as an artificial enzyme and efficient transmitter of electrons allowed reinforcing the relatively low catalytic activity of the immobilized natural enzymes that arises from changes in the nature of the enzyme and the slow electron transfer process between the enzyme and the electrode [86]. An example is the method recently developed by Nasiri et al. [76] for the determination of lactose (Figure 5), in which the natural enzyme cellobiose dehydrogenase (CDH) was immobilized on chitosan-coated magnetic nanoparticles and the bioconjugate was anchored on gC<sub>3</sub>N<sub>4</sub> sheets that acted as a direct electron transfer mediator to the electrode, thus increasing the electron transfer during the catalytic oxidation of lactose. The developed method allowed the determination of lactose in a 0.9 to 100 mM range with a detection limit of 0.3 mM and provided good results when applied to milk and dairy products.

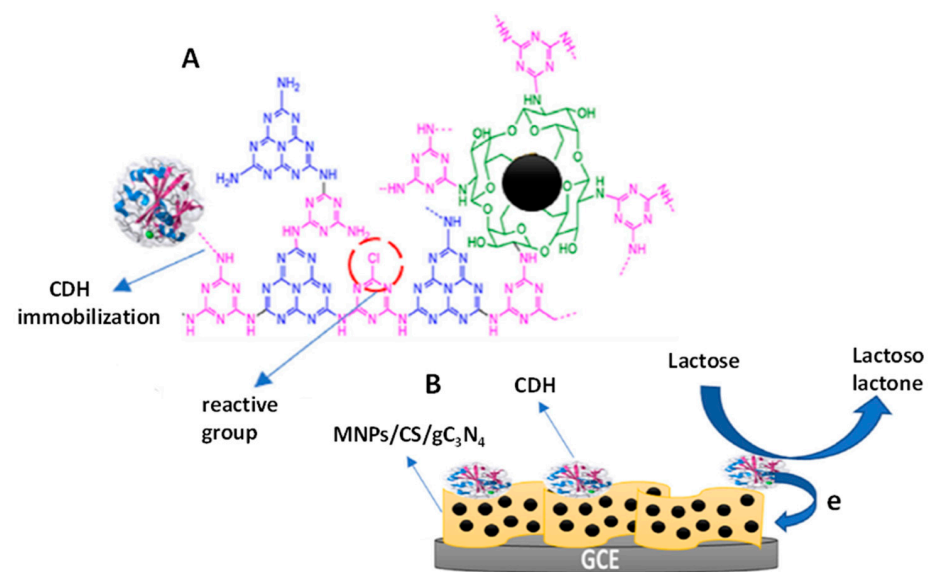


**Figure 5.** Schemes of (A) MNPs/CS/CDH/gC<sub>3</sub>N<sub>4</sub> and (B) the electrotransfer mechanism during lactose oxidation. Reprinted and adapted from [76] with permission.

Electrochemiluminescence (ECL) has increased the number of applications in the bio-sensing field due to its simplicity, low background, and high sensitivity [87]. Recent developments combining ECL with nanozyme amplification provide unique advantages for detection. For example, a cascade electrochemiluminescence (ECL) with integrated g-C<sub>3</sub>N<sub>4</sub> @ MOF nanozyme was prepared for the immunosensing of PSA [77]. As Figure 6 shows, luminol was loaded inside the nanozyme by encapsulation of MOF (NH<sub>2</sub>-MIL (53)-Fe) within g-C<sub>3</sub>N<sub>4</sub> nanosheets as a signal amplifier to label the detection antibody (Ab2). A sandwich-type immunosensing platform was developed with the capture antibody (Ab1) conjugated to magnetic nanoparticles (MNPs), providing ECL response in the presence of PSA. A calibration range of 0.1 pg mL<sup>-1</sup> to 60 ng mL<sup>-1</sup> and a high sensitivity were achieved with an LOD value of 0.02 pg mL<sup>-1</sup>. The good analytical performance was attributed to the high loading of luminol, the g-C<sub>3</sub>N<sub>4</sub> @ MOF catalyzed cascade enzymatic mimetic reaction, and the highly efficient electron transfer at the nanoporous gold electrode (NPGE). This same group prepared an ECL immuno-DNA biosensor for methylated DNA in which the target was sandwiched between anti-5-methylcytosine monoclonal antibody conjugated to MNPs (MNPs/anti-5mc) and luminol loaded within a phosphorylated DNA capture probe immobilized onto g-C<sub>3</sub>N<sub>4</sub> @ MOF (with MOF = UiO-66). In addition to the high signal amplification due to the nanozyme activity, this configuration showed a remarkable electrocatalytic activity of the rGO/pencil graphite electrode (PGE), providing a dynamic range from 20 pg to 20 ng with a detection limit of 10 pg [78].

Hybrids and nanocomposites of gC<sub>3</sub>N<sub>4</sub> have also been used for the preparation of photoelectrochemical (bio)sensors [88] due to the need for the use of stable artificial enzymes [89] and the additional property of this nanomaterial as a photocatalyst that makes it possible to design schemes of signal amplification achieving higher sensitivity. As is known, in these sensors, the current response is generated by excitation from an external radiation source, and it is measured on a transparent electrode such as fluorine-doped tin oxide (FTO). As an illustrative example of these applications, Zhu et al. [81] prepared a nanozyme composed of gold nanoparticles and Cu<sup>2+</sup>-modified boron nitride nanosheets (AuNPs/Cu<sup>2+</sup>-B-g C<sub>3</sub>N<sub>4</sub>) for the construction of a signal-off aptasensor for the assay of telomerase activity. As Figure 7 shows, an FTO electrode modified with Ag<sub>2</sub>S/AgNP-decorated ZnIn<sub>2</sub>S<sub>4</sub>/C<sub>3</sub>N<sub>4</sub> was used. Telomerase (TE) primer sequences (TS DNA) were extended by TE in the presence of deoxyribonucleoside triphosphates (dNTPs), which were bonded with the thiolated complementary DNA (cDNA). The nanozyme catalyzed the oxidation between 4-chloro-1-naphthol (4-CN) and H<sub>2</sub>O<sub>2</sub> to generate insoluble precipitation

on the photoelectrode, the inhibited signals with the TE-enabled TS extension allowing attaining a wide linear range of 50 to  $5 \times 10^5$  cells  $\text{mL}^{-1}$  and a low detection limit of 19 cells  $\text{mL}^{-1}$ .

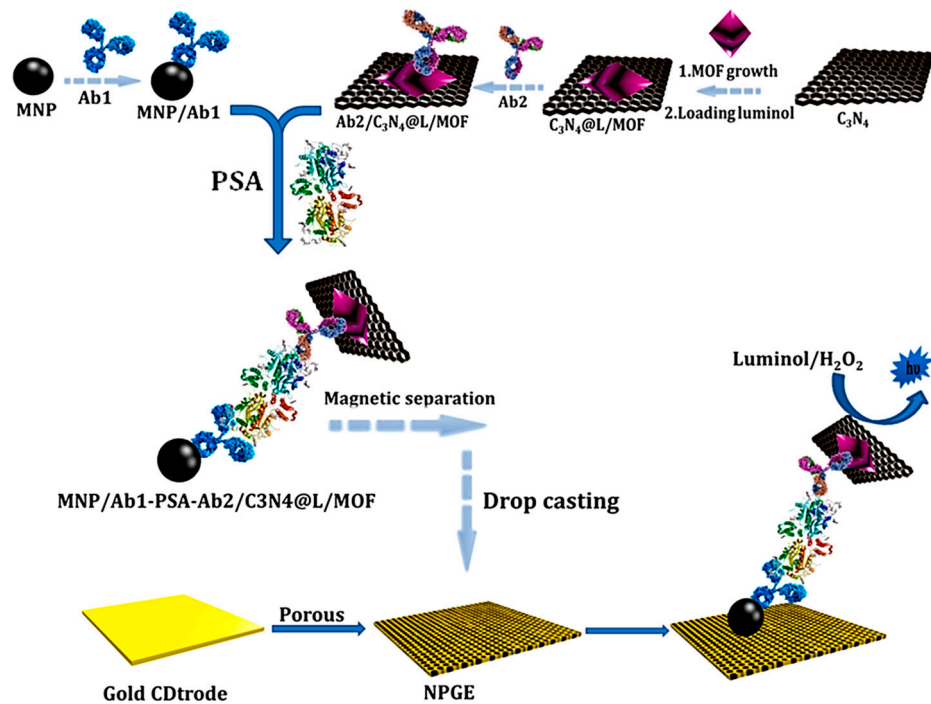


Figure 6. Amplified signal strategy based on the ECL-based nanozyme. Reprinted from [77] with permission.

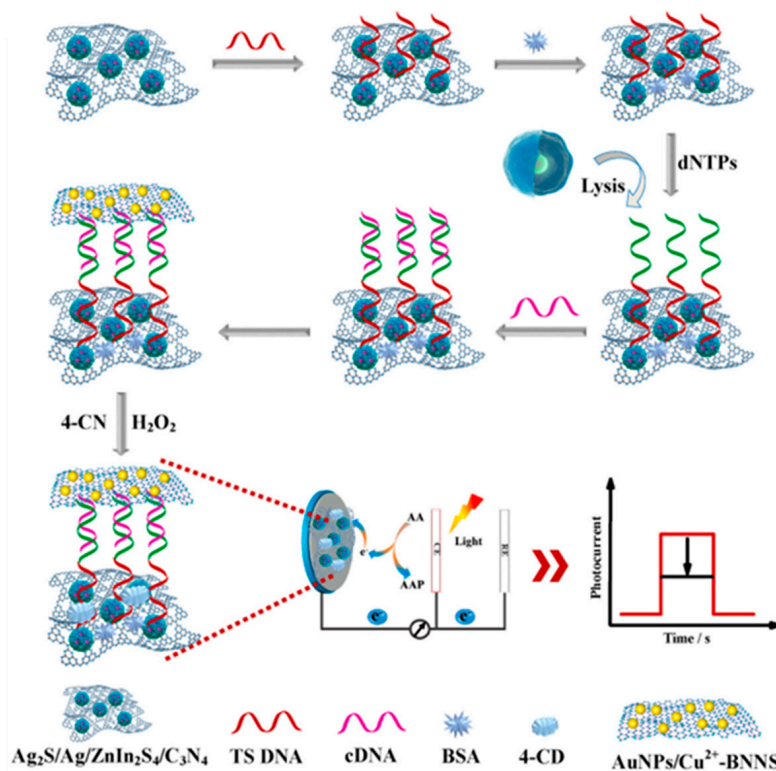


Figure 7. Schematic illustration of the photoelectrochemical biosensor developed for the determination of the telomerase activity. Reprinted from [81] with permission.

## 6. Conclusions and Prospects

Carbon nanozymes exhibit several properties that make them attractive for their use in electrochemical (bio)sensing. Their stability, high conductivity, and surface properties, along with low toxicity and biocompatibility, are some of the most valued features for the design of biosensing platforms. In addition, these nanomaterials can be easily modified by incorporating functional groups or biomolecules (antibodies, aptamers, or even natural enzymes) to improve selectivity, as well as preparing hybrid or composite nanomaterials that provide greater sensitivity, usually due to the increased catalytic activity. The properties of some carbon nanomaterials to act as artificial enzymes mimicking the role of natural peroxidases or oxidases provide an added value that makes them ideal for their use in environmental, food, or clinical fields, allowing the selective detection of target analytes in complex samples. Apart from all these advantages, it should be noted that currently, the preparation of these nanomaterials is cost-effective since the synthesis procedures are mostly environmentally friendly and adhere to the principles of green chemistry, using raw materials of natural origin and with minimal reagent consumption and waste production. However, the future increase in the use of carbon nanozymes and the improvement in their performance in (bio)sensing and, particularly, in (bio)sensing using electrochemical detection requires solving some problems and facing some of the challenges commented on below.

On the one hand, the preparation of carbon nanozymes with higher enzyme activity is an essential requirement. Indeed, in many cases, the artificial peroxidase or oxidase (the most common) role of these materials needs to be reinforced using less biocompatible and toxic metallic nanomaterials or even natural enzymes. In this sense, it is necessary to know the mechanisms by which the enzymatic activity is produced, since it can help to design more efficient nanomaterials. Furthermore, regarding electrochemical (bio)sensors, more research must be performed to clearly differentiate between electrocatalytic processes and those due to the enzymatic activity of the nanomaterial. In this sense, kinetic studies and verification of fitting to models such as the Michaelis–Menten type should be carried out. On the other hand, most of the developed methods involving carbon nanozymes use optical transduction based on the catalytic oxidation of TMB and colorimetric detection. However, despite the advantages of electrochemical detection, such as high sensitivity, low cost, portability, miniaturization capacity, and multiple analysis possibilities, the number of electrochemical biosensing methods using nanozymes is much smaller. An impulse should be given to these designs that involve the preparation of nanostructured electrode surfaces, making possible an efficient immobilization of reagents as well as developing strategies for signal amplification using nanozymes as labels or carrier tags, thus providing a more sensitive determination of analytes. Finally, the application of these (bio)sensors to real samples (clinical, environmental, or others) for the determination of the endogenous content of the target analytes in complex matrices is recommended to effectively validate the developed methods.

In summary, important issues and challenges still need to be solved to demonstrate the utility of carbon nanozymes in electroanalysis when facing real complex samples. These challenges should involve the development of new carbon nanomaterials with improved performance for analytical purposes as well as the development of methods of synthesis and preparation of composites and hybrids with enhanced enzyme activity able to allow the determination of endogenous species of interest at low concentration levels in complex real matrices.

**Author Contributions:** Writing—review and editing, P.Y.-S., E.S.-T. and J.M.P.; funding acquisition, P.Y.-S., E.S.-T. and J.M.P. All authors have read and agreed to the published version of the manuscript.

**Funding:** This research was funded by the Spanish Ministry of Science and Innovation, grant number PID2021-122457OB-I00.

**Data Availability Statement:** Not applicable.

**Conflicts of Interest:** The authors declare no conflict of interest. The funders had no role in the writing of the manuscript.

## References

1. Breslow, R.; Overman, L.E. An “Artificial Enzyme” combining a metal catalytic group and a hydrophobic binding cavity. *J. Am. Chem. Soc.* **1970**, *92*, 1075–1077. [[CrossRef](#)]
2. Smutok, O.; Kavetsky, T.; Prokopiv, T.; Serkiz, R.; Wojnarowska-Nowak, R.; Sausa, O.; Novak, D.; Berek, A.; Melman, M. Gonchar, New micro/nanocomposite with peroxidase-like activity in construction of oxidases-based amperometric biosensors for ethanol and glucose analysis. *Anal. Chim. Acta* **2021**, *1143*, 201–209. [[CrossRef](#)]
3. Das, B.; Lou Franco, J.; Logan, N.; Balasubramanian, P.; Kim, M.I.; Cao, C. Nanozymes in point-of-care diagnosis: An emerging futuristic approach for biosensing. *Nano-Micro. Lett.* **2021**, *13*, 193. [[CrossRef](#)] [[PubMed](#)]
4. Wu, Y.; Darland, D.C.; Zhao, J.X. Nanozymes—Hitting the Biosensing “Target”. *Sensors* **2021**, *21*, 5201. [[CrossRef](#)]
5. Arshad, F.; Arrigan, D.W.M.; Ahmed, M.U. Recent developments in nanozyme based sensors for detection of clinical bio-markers—A review. *IEEE Sens. J.* **2022**, *22*, 15. [[CrossRef](#)]
6. Wang, M.; Zhu, P.; Liu, S.; Chen, Y.; Liang, D.; Liu, Y.; Chen, W.; Du, L.; Wu, C. Application of nanozymes in environmental monitoring, management, and protection. *Biosensors* **2023**, *13*, 314. [[CrossRef](#)]
7. Wu, W.; Li, J. Recent progress on nanozymes in electrochemical sensing. *J. Electroanal. Chem.* **2023**, *936*, 117391. [[CrossRef](#)]
8. Wang, X.; Dong, S.; Wei, H. Recent advances on nanozyme-based electrochemical biosensors. *Electroanalysis* **2023**, *35*, 38–49. [[CrossRef](#)]
9. Tong, L.; Wu, L.; Su, E.; Li, Y.; Gu, N. Recent advances in the application of nanozymes in amperometric sensors, A Review. *Chemosensors* **2023**, *11*, 233. [[CrossRef](#)]
10. Sun, H.; Zhou, Y.; Ren, J.; Qu, X. Carbon nanozymes: Enzymatic properties, catalytic mechanism, and applications. *Angew. Chem. Int. Ed. Engl.* **2018**, *57*, 9224–9237. [[CrossRef](#)] [[PubMed](#)]
11. Dhiman, N.; Ghosh, S.; Mishra, Y.K.; Tripathi, K.M. Prospects of nano-carbons as emerging catalysts for enzyme-mimetic applications. *Mater. Adv.* **2022**, *3*, 3101–3122. [[CrossRef](#)]
12. Sun, Y.; Xu, B.; Pan, X.; Wang, H.; Wu, Q.; Li, S.; Jiang, B.; Liu, H. Carbon-based nanozymes: Design, catalytic mechanism, and bioapplication. *Coord. Chem. Rev.* **2023**, *475*, 214896. [[CrossRef](#)]
13. Wang, X.; Wang, H.; Zhou, S. Progress and perspective on carbon-based nanozymes for peroxidase-like applications. *J. Phys. Chem. Lett.* **2021**, *12*, 11751–11760. [[CrossRef](#)] [[PubMed](#)]
14. Ding, H.; Hu, B.; Zhang, B.; Zhang, H.; Yan, X.; Nie, G.; Liang, M. Carbon-based nanozymes for biomedical applications. *Nano Res.* **2021**, *14*, 570–583. [[CrossRef](#)]
15. Zhao, H.; Zhang, R.; Yan, X.; Fan, K. Superoxide dismutase nanozymes: An emerging star for anti-oxidation. *J. Mater. Chem. B* **2021**, *9*, 6939–6957. [[CrossRef](#)] [[PubMed](#)]
16. Dugan, L.L.; Gabrielsen, J.K.; Yu, S.P.; Lin, T.-S.; Choi, D.W. Buckminsterfullerenol free radical scavengers reduce excitotoxic and apoptotic death of cultured cortical neurons. *Neurobiol. Dis.* **1996**, *3*, 129–135. [[CrossRef](#)]
17. Ali, S.S.; Hardt, J.I.; Dugan, L.L. SOD activity of carboxyfullerenes predicts their neuroprotective efficacy: A structure-activity study. *Nanomed. NBM* **2008**, *4*, 283–294. [[CrossRef](#)]
18. Song, Y.; Wang, X.; Zhao, C.; Qu, K.; Ren, J.; Qu, X. Label-free colorimetric detection of single nucleotide polymorphism by using single-walled carbon nanotube intrinsic peroxidase-like activity. *Chem. Eur. J.* **2010**, *16*, 3617–3621. [[CrossRef](#)]
19. Wang, H.; Li, P.; Yu, D.; Zhang, Y.; Wang, Z.; Liu, C.; Qiu, H.; Liu, Z.; Ren, J.; Qu, X. Unraveling the enzymatic activity of oxygenated carbon nanotubes and their application in the treatment of bacterial infections. *Nano Lett.* **2018**, *18*, 3344–3351. [[CrossRef](#)]
20. Liu, Y.; Yan, X.; Tang, Y.; Lu, N.; Zhang, T.; Xu, Z.; Xing, Y.; Zhao, P.; Liu, M.; Zhu, Y.; et al. Cobalt nanoparticles decorated bamboo-like N-doped carbon nanotube as nanozyme sensor for efficient biosensing. *J. Electroanal. Chem.* **2022**, *926*, 116932. [[CrossRef](#)]
21. Liao, Y.; Liu, J.; Liu, M.; Lin, L.; Wang, X.; Quan, Z. Iron nanoparticles encapsulated in boron-nitrogen Co-doped carbon nanotubes biomimetic enzyme for electrochemical monitoring of dopamine and uric acid in human serum. *Microchem. J.* **2023**, *185*, 108184. [[CrossRef](#)]
22. Gallay, P.; Eguílaz, M.; Rivas, G. Designing electrochemical interfaces based on nanohybrids of avidin functionalized-carbon nanotubes and ruthenium nanoparticles as peroxidase-like nanozyme with supramolecular recognition properties for site-specific anchoring of biotinylated residues. *Biosens. Bioelectron.* **2020**, *148*, 111764. [[CrossRef](#)]
23. Lin, S.-Y.; Lin, C.-Y. Electrochemically-functionalized CNT/ABTS nanozyme enabling sensitive and selective voltammetric detection of microalbuminuria. *Anal. Chim. Acta* **2022**, *1197*, 339517. [[CrossRef](#)]
24. Zhu, X.; Liu, P.; Ge, Y.; Wu, R.; Xue, T.; Sheng, Y.; Ai, S.; Tang, K.; Wei, Y. MoS<sub>2</sub>/MWCNTs porous nanohybrid network with oxidase-like characteristic as electrochemical nanozyme sensor coupled with machine learning for intelligent analysis of car-bendazim. *J. Electroanal. Chem.* **2020**, *862*, 113940. [[CrossRef](#)]
25. Feng, L.; Zhang, L.; Chu, S.; Zhang, S.; Chen, X.; Gong, Y.; Du, Z.; Mao, G.; Wang, H. One-pot fabrication of nanozyme with 2D/1D heterostructure by in-situ growing MoS<sub>2</sub> nanosheets onto single-walled carbon nanotubes with enhanced catalysis for colorimetric detection of glutathione. *Anal. Chim. Acta* **2022**, *1221*, 340083. [[CrossRef](#)] [[PubMed](#)]

26. Arévalo, B.; Blázquez-García, M.; Valverde, A.; Serafín, V.; Montero, A.; Solis, G.; Barderas, R.; Campuzano, S.; Yáñez-Sedeño, P.; Pingarrón, J.M. Binary MoS<sub>2</sub> nanostructures as nanocarriers for amplification in multiplexed electrochemical immunosensing: Simultaneous determination of B cell activation factor and proliferation-induced signal immunity-related cytokines. *Microchim. Acta* **2022**, *189*, 143. [[CrossRef](#)]
27. Song, Y.; Qu, K.; Zhao, C.; Ren, J.; Qu, X. Graphene oxide: Intrinsic peroxidase catalytic activity and its application to glucose detection. *Adv. Mater.* **2010**, *22*, 2206–2210. [[CrossRef](#)]
28. Wang, D.; Song, X.; Li, P.; Gao, X.J.; Gao, X. Origins of the peroxidase mimicking activities of graphene oxide from first principles. *J. Mater. Chem. B* **2020**, *8*, 9028–9034. [[CrossRef](#)]
29. Lou, Z.; Zhao, S.; Wang, Q.; Wei, H. N-doped carbon as peroxidase-like nanozymes for total antioxidant capacity assay. *Anal. Chem.* **2019**, *91*, 15267–15274. [[CrossRef](#)]
30. Hu, Y.; Gao, X.J.; Zhu, Y.; Muhammad, F.; Tan, S.; Cao, W.; Lin, S.; Jin, Z.; Gao, X.; Wei, H. Nitrogen-doped carbon nanomaterials as highly active and specific peroxidase mimics. *Chem. Mater.* **2018**, *30*, 6431–6439. [[CrossRef](#)]
31. Dilmac, Y.; Guler, M. Fabrication of non-enzymatic glucose sensor dependent upon Au nanoparticles deposited on carboxylated graphene oxide. *J. Electroanal. Chem.* **2020**, *864*, 114091. [[CrossRef](#)]
32. Li, G.; Wang, B.; Li, L.; Li, X.; Yan, R.; Liang, J.; Zhou, X.; Li, L.; Zhou, Z. H-rGO-Pd NPs nanozyme enhanced silver deposition strategy for electrochemical detection of glypican-3. *Molecules* **2023**, *28*, 2271. [[CrossRef](#)] [[PubMed](#)]
33. Lu, N.; Liu, Y.; Yan, Z.; Xu, Z.; Xing, Y.; Song, Y.; Zhao, P.; Liu, M.; Gu, Y.; Zhang, Z.; et al. Bioinspired surface modification of graphene-based hybrids as nanozyme sensors for simultaneous detection of dopamine and uric acid. *ACS Appl. Nano Mater.* **2022**, *5*, 11361–11370. [[CrossRef](#)]
34. Gugoasa, L.A.D.; Pogacean, F.; Kurbanoglu, S.; Tudoran, L.B.; Serban, A.B.; Kacso, I.; Prunea, S. Graphene-gold nanoparticles nanozyme-based electrochemical sensor with enhanced laccase-like activity for determination of phenolic substrates. *J. Electrochem. Soc.* **2021**, *168*, 067523. [[CrossRef](#)]
35. Dinu, L.A.; Kurbanoglu, S.; Romanitan, C.; Pruneanu, S.; Serban, A.B.; Stoian, M.C.; Pachiu, C.; Craciun, G. Electrodeposited copper nanocubes on multi-layer graphene: A novel nanozyme for ultrasensitive dopamine detection from biological samples. *Appl. Surf. Sci.* **2022**, *604*, 154392. [[CrossRef](#)]
36. Zhang, Y.; Pershina, L.; Kudriashov, D.; Offenhausser, A.; Mourzina, Y. Influence of the chemically reduced graphene oxide interface on the antioxidant multienzyme properties of Prussian blue nanoparticles. *Coll. Interf. Sci. Commun.* **2023**, *52*, 100689. [[CrossRef](#)]
37. Zhu, Y.; Liu, P.; Xue, T.; Xu, J.; Qiu, D.; Sheng, Y.; Li, W.; Lu, X.; Ge, Y.; Wen, Y. Facile and rapid one-step mass production of flexible 3D porous graphene nanozyme electrode via direct laser-writing for intelligent evaluation of fish freshness. *Microchem. J.* **2021**, *162*, 105855. [[CrossRef](#)]
38. Li, G.; Wu, G.; Huang, J.; Wang, B.; Li, H.M.; Chen, W.; Liang, J.; Tan, M.; Zhou, Z. Nanozyme-mediated cascade reaction system for electrochemical detection of 1,5-anhydroglucitol. *Bioelectrochemistry* **2022**, *147*, 108204. [[CrossRef](#)]
39. Zhang, T.; Liu, Y.; Pi, J.; Lu, N.; Zhang, R.; Chen, W.; Zhang, Z.; Xing, D. A novel artificial peroxisome candidate based on nanozyme with excellent catalytic performance for biosensing. *Biosens. Bioelectron.* **2022**, *196*, 113686. [[CrossRef](#)]
40. Yao, X.; Liu, T.; Xie, Y.; Chu, Z.; Jin, W. In situ-forming magnetic Fe<sub>3</sub>O<sub>4</sub> nanoroses on defect-controllable mesoporous graphene oxide for enzyme-mimic sensing. *Ind. Eng. Chem. Res.* **2020**, *59*, 17934–17943. [[CrossRef](#)]
41. Savas, S.; Altintas, Z. Graphene quantum dots as nanozymes for electrochemical sensing of *Yersinia enterocolitica* in milk and human serum materials. *Materials* **2019**, *12*, 2189. [[CrossRef](#)] [[PubMed](#)]
42. Facure, M.H.M.; Andre, R.S.; Cardoso, R.M.; Mercante, L.A.; Correa, D.S. Electrochemical and optical dual-mode detection of phenolic compounds using MnO<sub>2</sub>/GQD nanozyme. *Electrochim. Acta* **2023**, *441*, 141777. [[CrossRef](#)]
43. Stefanov, C.; Negut, C.C.; Gugoasa, L.A.D.; van Staden, J.F. Gold nanoparticle-graphene quantum dots nanozyme for the wide range and sensitive electrochemical determination of quercetin in plasma droplets. *Microchim. Acta* **2020**, *187*, 611. [[CrossRef](#)]
44. Zamani, M.; Tavakkoli, N.; Soltani, N. Electrochemical sensor based on graphene quantum dot/gold nanoparticles and thiol-containing organic compound for measuring methotrexate anti-cancer drug. *Diam. Relat. Mater.* **2023**, *136*, 109954. [[CrossRef](#)]
45. Zhang, Y.; Wei, X.; Gao, Q.; Zhang, J.; Ding, Y.; Xue, L.; Chen, M.; Wang, J.; Wu, S.; Yang, X.; et al. Cascade amplification based on PEI-functionalized metal-organic framework supported gold nanoparticles/nitrogen-doped graphene quantum dots for amperometric biosensing applications. *Electrochim. Acta* **2022**, *405*, 139803. [[CrossRef](#)]
46. Mansuriya, B.D.; Altintas, Z. Enzyme-free electrochemical nano-immunosensor based on graphene quantum dots and gold nanoparticles for cardiac biomarker determination. *Nanomaterials* **2021**, *11*, 578. [[CrossRef](#)]
47. Zhang, D.; Han, Q.; Liu, W.; Xu, K.; Shao, M.; Li, Y.; Du, P.; Zhang, Z.; Liu, B.; Zhang, L.; et al. Au-decorated N-rich carbon dots as peroxidase mimics for the detection of acetylcholinesterase activity. *ACS Appl. Nano Mater.* **2022**, *5*, 1958–1965. [[CrossRef](#)]
48. Cao, X.; Liu, M.; Lu, J.; Lv, H.; Han, J.; He, S.; Ye, Y.; Chen, X.; Wei, Z.; Zheng, H. An ultrasensitive biosensor for virulence ompA gene of *Cronobacter sakazakii* based on boron doped carbon quantum dots-AuNPs nanozyme and exonuclease III-assisted target-recycling strategy. *Food Chem.* **2022**, *391*, 133268. [[CrossRef](#)]
49. Jiang, G.; Liu, H.; Liu, J.; Liu, L.; Li, Y.; Xue, L.; Wu, Y.; Yang, R. Engineering of multifunctional carbon nanodots-decorated plasmonic Au@Ag nanozymes for photoelectrochemical biosensing of microRNA-155. *Sens. Actuators B* **2022**, *360*, 131653. [[CrossRef](#)]

50. Li, S.; Pang, C.; Ma, X.; Zhang, Y.; Xu, Z.; Li, J.; Zhang, M.; Wang, M. Microfluidic paper-based chip for parathion-methyl detection based on a double catalytic amplification strategy. *Microchim. Acta* **2021**, *188*, 438. [[CrossRef](#)]
51. Sridara, T.; Upan, J.; Saianand, G.; Tuantranont, A.; Karuwan, C.; Jakmunee, J. Non-enzymatic amperometric glucose sensor based on carbon nanodots and copper oxide nanocomposites electrode. *Sensors* **2020**, *20*, 808. [[CrossRef](#)]
52. Honarasa, F.; Keshkar, S.; Eskandari, N.; Eghbal, M. Catalytic and electrocatalytic activities of Fe<sub>3</sub>O<sub>4</sub>/CeO<sub>2</sub>/C-dot nanocomposite. *Chem. Pap.* **2021**, *75*, 2371–2378. [[CrossRef](#)]
53. Li, S.; Pang, E.; Li, N.; Chang, Q.; Yang, J.; Hu, S. A bifunctional nanozyme of carbon dots-mediated Co<sub>9</sub>S<sub>8</sub> formation. *J. Coll. Interf. Sci.* **2022**, *608*, 1348–1354. [[CrossRef](#)] [[PubMed](#)]
54. Li, Z.; Deng, X.; Hong, X.; Zhao, S. Nanozyme based on dispersion of hemin by graphene quantum dots for colorimetric detection of glutathione. *Molecules* **2022**, *27*, 6779. [[CrossRef](#)]
55. Lee, A.; Kang, W.; Choi, J.S. Highly enhanced enzymatic activity of Mn-Induced carbon dots and their application as colorimetric sensor probes. *Nanomaterials* **2021**, *11*, 3046. [[CrossRef](#)] [[PubMed](#)]
56. Bavykina, A.; Kolobov, N.; Khan, I.S.; Bau, J.A.; Ramirez, A.; Gascon, J. Metal-organic frameworks in heterogeneous catalysis: Recent progress, new trends, and future perspectives. *Chem. Rev.* **2020**, *120*, 8468–8535. [[CrossRef](#)]
57. Zhang, Y.; Li, B.; Wei, X.; Gu, Q.; Chen, M.; Zhang, J.; Mo, S.; Wang, J.; Xue, L.; Ding, Y.; et al. Amplified electrochemical antibiotic aptasensing based on electrochemically deposited AuNPs coordinated with PEI-functionalized Fe-based metal-organic framework. *Microchim. Acta* **2021**, *188*, 286. [[CrossRef](#)]
58. López-Cantu, J.O. González-González, R.B.; Melchor-Martínez, E.M.; Hernández Martínez, S.A.; Araújo, R.G.; Parra-Arroyo, L.; Sosa-Hernández, J.E.; Parra-Saldívar, R.; Iqbal, H.M.N. Enzyme-mimicking capacities of carbon-dots nanozymes: Properties, catalytic mechanism, and applications—A review. *Int. J. Biol. Macromol.* **2022**, *194*, 676–687.
59. Jin, J.; Li, L.; Zhang, L.; Luan, Z.; Xin, S.; Song, K. Progress in the application of carbon dots-based nanozymes. *Front. Chem.* **2021**, *9*, 748044. [[CrossRef](#)] [[PubMed](#)]
60. He, D.; Yan, M.; Sun, P.; Sun, Y.; Qu, L.; Li, Z. Recent progress in carbon-dots-based nanozymes for chemosensing and biomedical applications. *Chin. Chem. Lett.* **2021**, *32*, 2994–3006. [[CrossRef](#)]
61. Lu, C.; Chen, X. Nanostructure engineering of graphitic carbon nitride for electrochemical applications. *ACS Nano* **2021**, *15*, 18777–18793. [[CrossRef](#)] [[PubMed](#)]
62. Umaphathi, R.; Raju, C.V.; Ghoreishian, S.; Rani, G.M.; Kumar, K.; Oh, M.H.; Park, J.P.; Huh, Y.-S. Recent advances in the use of graphitic carbon nitride-based composites for the electrochemical detection of hazardous contaminants. *Coord. Chem. Rev.* **2022**, *470*, 214708. [[CrossRef](#)]
63. Xiao, F.; Li, H.; Yan, X.; Yan, L.; Zhang, X.; Wang, M.; Qian, C.; Wang, Y. Graphitic carbon nitride/graphene oxide (g-C<sub>3</sub>N<sub>4</sub>/GO) nanocomposites covalently linked with ferrocene containing dendrimer for ultrasensitive detection of pesticide. *Anal. Chim. Acta* **2020**, *1103*, 84–96. [[CrossRef](#)] [[PubMed](#)]
64. Talukdar, M.; Deb, P. Recent progress in research on multifunctional graphitic carbon nitride: An emerging wonder material beyond catalyst. *Carbon* **2022**, *192*, 308–331. [[CrossRef](#)]
65. Vinoth, S.; Shalini Devi, K.S.; Pandikumar, A. A comprehensive review on graphitic carbon nitride based electrochemical and biosensors for environmental and healthcare applications. *Trends Anal. Chem.* **2021**, *140*, 116274. [[CrossRef](#)]
66. Kurup, C.P.; Ahmed, M.U. Nanozymes towards personalized diagnostics: A recent progress in biosensing. *Biosensors* **2023**, *13*, 461. [[CrossRef](#)]
67. Mei, L.; Zhu, S.; Liu, Y.; Yin, W.; Gu, Z.; Zhao, Y. An overview of the use of nanozymes in antibacterial applications. *Chem. Eng. J.* **2021**, *418*, 129431. [[CrossRef](#)]
68. Borthakur, P.; Boruah, P.K.; Das, M.R. Facile synthesis of CuS nanoparticles on two-dimensional nanosheets as efficient artificial nanozyme for detection of Ibuprofen in water. *J. Environ. Chem. Eng.* **2021**, *9*, 104635. [[CrossRef](#)]
69. Zeng, G.; Duan, M.; Xu, Y.; Ge, F.; Wang, W. Platinum (II)-doped graphitic carbon nitride with enhanced peroxidase-like activity for detection of glucose and H<sub>2</sub>O<sub>2</sub>. *Spectrochim. Acta A* **2020**, *241*, 118649. [[CrossRef](#)]
70. Jin, X.; Chen, J.; Zeng, X.; Xu, L.; Wu, Y.; Fu, F. A signal-on magnetic electro-chemical immunosensor for ultra-sensitive detection of saxitoxin using palladium-doped graphitic carbon nitride-based non-competitive strategy. *Biosens. Bioelectron.* **2019**, *128*, 45–51. [[CrossRef](#)]
71. Gupta, N.; Todi, K.; Narayan, T.; Malhotra, B.D. Graphitic carbon nitride-based nanoplatfoms for biosensors: Design strategies and applications. *Mater. Today Chem.* **2022**, *24*, 100770. [[CrossRef](#)]
72. Yang, G.; Chen, Y.; Shi, R.; Chen, R.; Gao, S.; Zhang, S.; Rao, Y.; Lu, Y.; Peng, Y.; Qing, Z.; et al. Platinum nanoparticles loaded graphitic carbon nitride nanosheets with enhanced peroxidase-like activity for H<sub>2</sub>O<sub>2</sub> and oxidase-based sensing. *Molecules* **2023**, *28*, 3736. [[CrossRef](#)] [[PubMed](#)]
73. Zhu, W.; Hao, N.; Lu, J.; Dai, Z.; Qian, J.; Yang, X.; Wang, K. Highly active metal-free peroxidase mimics based on oxygen-doped carbon nitride by promoting electrotransfer capacity. *Chem. Commun.* **2020**, *56*, 1409. [[CrossRef](#)] [[PubMed](#)]
74. Imran, H.; Vaishali, K.; Francy, S.A.; Manikandan, P.N.; Dharuman, V. Platinum and zinc oxide modified carbon nitride electrode as non-enzymatic highly selective and reusable electrochemical diabetic sensor in human blood. *Bioelectrochemistry* **2021**, *137*, 107645. [[CrossRef](#)] [[PubMed](#)]

75. Li, M.; He, B. Ultrasensitive sandwich-type electrochemical biosensor based on octahedral gold nanoparticles modified poly (ethylenimine) functionalized graphitic carbon nitride nanosheets for the determination of sulfamethazine. *Sens. Actuators B* **2021**, *329*, 129158. [[CrossRef](#)]
76. Nasiri, H.; Baghban, H.; Teimuri-Mofrad, R.; Mokhtarzadeh, A. Graphitic carbon nitride/magnetic chitosan composite for rapid electrochemical detection of lactose. *Int. Dairy J.* **2023**, *136*, 10548. [[CrossRef](#)]
77. Khoshfetrat, S.M.; Hashemi, P.; Afkhami, A.; Hajian, A.; Bagheri, H. Cascade electrochemiluminescence-based integrated graphitic carbon nitride-encapsulated metal-organic framework nanozyme for prostate-specific antigen biosensing. *Sens. Actuators B* **2021**, *348*, 130658. [[CrossRef](#)]
78. Khoshfetrat, S.M.; Dorraji, P.S.; Fotouhi, L.; Hosseini, M.; Khatami, F.; Moazami, H.R.; Omidfar, K. Enhanced electrochemiluminescence biosensing of gene-specific methylation in thyroid cancer patients' plasma based integrated graphitic carbon nitride-encapsulated metal-organic framework nanozyme optimized by central composite design. *Sens. Actuators B* **2022**, *364*, 131895. [[CrossRef](#)]
79. Hari Krishnan, K.; Singh, G.; Kushwaha, A.; Singh, V.P.; Gaur, U.K.; Sharma, M. 2D/2D heterojunction of graphitic carbon nitride and hexagonal boron nitride nanosheets mediated electrochemical detection of hazardous hydroquinone with high selectivity and sensitivity. *J. Environ. Chem. Eng.* **2022**, *10*, 108717. [[CrossRef](#)]
80. Murugan, R.; Hwa, K.Y.; Santhan, A. 2D-graphitic carbon nitride nanosheet/metal nanocomposites for electrochemical sensor of hydroquinone in real sample analysis. *ACS Appl. Nano Mater.* **2023**, *6*, 8550–8563. [[CrossRef](#)]
81. Zhu, J.-H.; Gou, H.; Zhao, T.; Mei, L.-P.; Wang, A.-J.; Feng, J.-J. Ultrasensitive photoelectrochemical aptasensor for detecting telomerase activity based on Ag<sub>2</sub>S/Ag decorated ZnIn<sub>2</sub>S<sub>4</sub>/C<sub>3</sub>N<sub>4</sub> 3D/2D Z-scheme heterostructures and amplified by Au/Cu<sup>2+</sup>-boron-nitride nanozyme. *Biosens. Bioelectron.* **2022**, *203*, 114048. [[CrossRef](#)] [[PubMed](#)]
82. Zhang, K.; Lv, S.; Zhou, Q.; Tang, D. CoOOH nanosheets-coated g-C<sub>3</sub>N<sub>4</sub>/CuInS<sub>2</sub> nanohybrids for photoelectrochemical biosensor of carcinoembryonic antigen coupling hybridization chain reaction with etching reaction. *Sens. Actuators B* **2020**, *307*, 127631. [[CrossRef](#)]
83. Deveci, H.A.M.; Kaya, M.; Kaya, I.; Yola, B.B.; Atar, N.; Yola, M.L. Bisphenol A imprinted electrochemical sensor based on graphene quantum dots with boron functionalized g-C<sub>3</sub>N<sub>4</sub> in food samples. *Biosensors* **2023**, *13*, 725. [[CrossRef](#)] [[PubMed](#)]
84. Nirbhaya, V.; Chauhan, D.; Jain, R.; Chandra, R.; Kumar, S. Nanostructured graphitic carbon nitride based ultrasensing electrochemical biosensor for food toxin detection. *Bioelectrochemistry* **2021**, *139*, 107738. [[CrossRef](#)]
85. Gowri, V.M.; John, S.A. Fabrication of bulk, nanosheets and quantum dots of graphitic carbon nitride on electrodes: Morphology dependent electrocatalytic activity. *J. Electroanal. Chem.* **2021**, *895*, 115474. [[CrossRef](#)]
86. Varmira, K.; Mohammadi, G.; Mahmoudi, M.; Khodarahmi, R.; Rashidi, K.; Hedayati, M.; Goicoechea, H.C.; Javaland, A.R. Fabrication of a novel enzymatic electrochemical biosensor for determination of tyrosine in some food samples. *Talanta* **2018**, *183*, 1–10. [[CrossRef](#)]
87. Fiorani, A.; Merino, J.P.; Zanutt, A.; Criado, A.; Valenti, G.; Prato, M.; Paolucci, F. Advanced carbon nanomaterials for electrochemiluminescent biosensor applications. *Curr. Op. Electrochem.* **2019**, *16*, 66–74. [[CrossRef](#)]
88. Fu, J.; Yu, J.; Jiang, C.; Cheng, B. g-C<sub>3</sub>N<sub>4</sub>-based heterostructured photocatalysts. *Adv. Energ. Mat.* **2018**, *8*, 1701503. [[CrossRef](#)]
89. Wang, P.; Cao, L.; Chen, Y.; Wu, Y.; Di, J. Photoelectrochemical biosensor based on Co<sub>3</sub>O<sub>4</sub> nanoenzyme coupled with PbS quantum dots for hydrogen peroxide detection. *ACS Appl. Nano Mater.* **2019**, *2*, 2204–2211. [[CrossRef](#)]

**Disclaimer/Publisher's Note:** The statements, opinions and data contained in all publications are solely those of the individual author(s) and contributor(s) and not of MDPI and/or the editor(s). MDPI and/or the editor(s) disclaim responsibility for any injury to people or property resulting from any ideas, methods, instructions or products referred to in the content.